-RESEARCH PAPER-

International Journal of Mining and Geo-Engineering

IJMGE

IJMGE 60-2 (2026) 139-148

DOI:10.22059/IJMGE.2026.398627.595278

Integrated petrographic and XRD characterization of carboniferous-aged sandstones from the Zonguldak basin (NW Turkey): insights into tectonic provenance and sedimentary processes

Zikrullah Samet Güloğlu [a, *], Çağrı Aldi [a], Halil Bölük [a] and Olgay Yarali [b]

[a] *Department of Mining and Mineral Extraction, Caycuma Vocational School, Zonguldak Bulent Ecevit University, Zonguldak, Türkiye.*

[b] *Department of Mining Engineering, Faculty of Engineering, Zonguldak Bulent Ecevit University, Zonguldak, Türkiye.*

Article History:

Received: 15 July 2025.

Revised: 08 November 2025.

Accepted: 03 May 2026.

ABSTRACT

This study presents an integrated petrographic and mineralogical evaluation of Carboniferous-aged sandstone units from the Zonguldak Basin, located in northwestern Turkey. A total of four representative samples from the Kozlu, Armutçuk, Üzülmez, and Karadon formations were analyzed through thin-section petrography and X-ray Diffraction (XRD) techniques to investigate their compositional characteristics, provenance signatures, and depositional environments. Petrographic analysis revealed that the majority of the samples fall into Feldspathic Litharenite, Arkose and Lithic Arkose categories, based on Folk's sandstone classification scheme. The dominance of quartz and feldspar, alongside lithic fragments derived from felsic igneous and high-grade metamorphic sources, suggests deposition under tectonically active conditions with limited chemical weathering and short sediment transport distances. XRD analyses confirmed the presence of quartz, feldspar, clay minerals (illite, muscovite), and minor calcite. The diffraction patterns exhibit sharp peaks for quartz and feldspar, indicating well-crystallized detrital grains, whereas broader peaks for clay minerals imply diagenetic alteration during burial. Grain size assessments indicate a wide spectrum ranging from fine- to coarse-grained textures, which points to fluctuating depositional energies—likely controlled by fluvio-deltaic processes in an actively uplifting basin margin. The presence of angular lithic fragments and feldspar-rich assemblages supports a provenance associated with nearby orogenic highlands. These findings are consistent with previous tectonic reconstructions that associate the Zonguldak Basin with the closure of the Intrapontide Ocean and collisional events during the Paleozoic–Mesozoic transition. Overall, this study provides significant insights into the sedimentary and tectonic evolution of the Zonguldak Basin and contributes to a better understanding of the basin's geodynamic history and sedimentary processes.

Keywords: *Zonguldak Basin, tectonic provenance, sandstone petrography, mineralogical analysis, x-ray diffraction (XRD).*

GRAPHICAL ABSTRACT

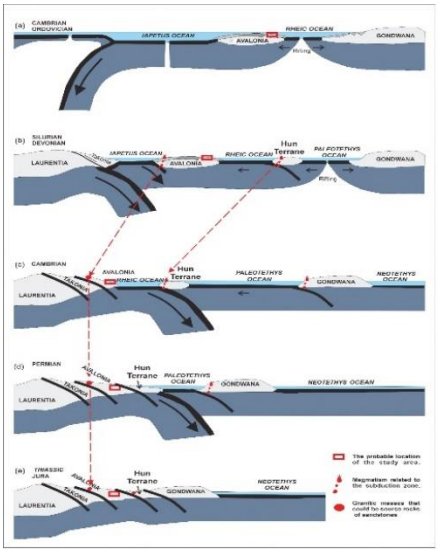

* Corresponding author. *E-mail address:* : sametguloglu610@gmail.com (Z. S. Güloğlu).

1. Introduction

The Zonguldak Basin, as Turkey's only hard coal basin, is part of the Pontide tectonic unit and corresponds to the avant-fosse (foredeep) section of the Alpine orogenic belt [1]. The basin represents a unique geological setting that provides crucial insights into the Paleozoic-Mesozoic tectonic evolution of the western Pontides and the broader Tethyan realm. The tectonic evolution of the basin began primarily during the Cretaceous period and became more pronounced due to post-Cretaceous movements. The unconformity between Carboniferous and Cretaceous-aged strata is a direct result of these tectonic activities.

The geological significance of the Zonguldak Basin extends beyond its economic importance as Turkey's sole hard coal producer. The basin serves as a natural laboratory for understanding foreland basin evolution, sediment provenance relationships, and the impact of orogenic processes on sedimentary systems. The Carboniferous coal-bearing sequences represent a critical time period when global climate changes, sea-level fluctuations, and tectonic movements converged to create optimal conditions for organic matter accumulation and preservation.

During the post-Cretaceous movements, it has been observed that rigid limestone layers and more ductile shale, graywacke, and conglomerate series experienced different types of deformation. In this process, a significant fault, known as the "Midi Fault," was formed, delineating the southern boundary of the basin. South of this fault, the Alacaağzı series is characterized by steep or overturned bedding, whereas further south, the Cretaceous cover strata obscure this structure. Therefore, it is hypothesized that regularly folded productive Carboniferous series may exist beneath the cover sequences [1].

The structural complexity of the basin has profound implications for both scientific understanding and practical applications. The heterogeneous deformation patterns observed across different lithological units reflect the varying rheological properties of sedimentary rocks under stress, providing insights into the mechanical behavior of foreland basin sequences during orogenic loading.

The tectonic structure of the basin has led to heterogeneities in the thickness and dip of coal seams, creating challenges for mining activities. The intense tectonic effects have contributed to the irregular distribution of seams and an increase in the amount of firedamp. As a result, full mechanization applications in the basin have remained limited, and production has predominantly been carried out using labour-intensive methods [1].

The sedimentary units outcropping in the basin are divided into two main formations of different ages: Carboniferous and Cretaceous. The Carboniferous-aged units form the basement rocks that host the region's hard coal deposits, whereas the Cretaceous-aged units unconformably overlie these formations as cover rocks [2]. Both formations contain significant psammitic (sandstone) and psephitic (conglomerate) rock types. However, the limited fossil content of these rocks increases the importance of lithological comparisons [3]. During the Carboniferous period, particularly in the Westphalian stage (approximately 315–305 million years ago), more than 20 coal-bearing horizons were formed in the basin [4]. During this time, as the sea regressed, the uplift of the southern landmass intensified, leading to the development of high-energy fluvial systems. Consequently, coarse-grained conglomerates and coarse sandstones were deposited sequentially with fine-grained floodplain sediments such as claystone and siltstone, representing more quiescent depositional conditions.

It was stated [5] that during the Middle Paleozoic, the Zonguldak Basin was located along the southern margin of the Laurasian plate and was subjected to significant tectonic movements during the Hercynian orogeny. Throughout this process, E-NE/W-SW trending faults and folds developed within the basin, leading to the tilting of Paleozoic sedimentary units. The Hercynian orogeny resulted from the collision between the Laurasia and Gondwana continents, profoundly influencing the structural characteristics of the basin. The tectonic movements of this period contributed to the formation of the angular unconformity observed above the Karadon Formation. During the Cretaceous period, the Zonguldak Basin experienced a general phase of subsidence, rifting, and faulting [2]. These tectonic activities facilitated the deposition of new sedimentary sequences and led to the faulting of coal seams in the region. Additionally, during the Aptian stage, the subduction of the Intrapontide Ocean triggered the opening of the Black Sea as a back-arc basin, marking the onset of the Alpine orogeny. The andesitic volcaniclastic sediments of the Yemişliçay Formation from this period further support the subduction of oceanic crust in the region. In the Eocene, the collision between the Western Pontide and Eastern Pontide tectonic domains resulted in the cessation of the Intrapontide Ocean's subduction, leading to the uplift of the Zonguldak Basin. These tectonic movements halted sedimentary deposition in the basin and contributed to the formation of its present-day structural characteristics. Due to the influence of the Alpine orogeny, a progressive uplift process was observed, causing the exposure of older sedimentary units, particularly in the northern parts of the basin.

The tectonic structure of the basin has become complex due to the influence of Hercynian and Alpine orogenic movements. These tectonic processes have led to the folding and faulting of rock units in the region, resulting in the fragmentation of formations into discontinuous units [5]. This structural complexity poses significant challenges for coal exploration and mining operations [2].

The geological evolution of the Zonguldak Basin has played a critical role in the region's economic and industrial development. The formation and distribution of coal deposits are directly related to the geological and tectonic history of the basin. Therefore, a detailed examination of the basin's geological characteristics is of great significance for both academic research and mining activities. Within this scope, modal analyses were conducted on samples collected from the Kozlu, Armutçuk, Üzülmez, and Karadon regions [6] (Figure 1). These analyses determined the mineralogical compositions, textural characteristics, and grain size distributions of the rock units. The primary objective of this study is to investigate the mineralogical and petrographic properties of sandstone samples from the Zonguldak Basin and to provide insights into the region's tectonic and sedimentary evolution.

2. Materials and Methods

Systematic sampling was conducted in the Zonguldak Basin, specifically from the Kozlu, Armutçuk, Üzülmez, and Karadon regions. Thin sections were prepared at the Istanbul Technical University, Faculty of Mines laboratory. Modal percentages of framework grains were determined by point-counting 400 points per thin section using standard petrographic microscopy techniques following the Gazzi-Dickinson method [8, 7]. All values have been recalculated and normalized to 100% to represent framework grain composition only, excluding matrix and cement. Modal analyses were performed on 14 samples, and the results are presented in Table 1.

Additionally, X-Ray Diffraction (XRD) pattern analysis (standard analysis) was conducted on four selected samples (AR-1, KA-1, KO-2, and U-4) at the Science and Technology Application and Research Center (ARTMER) of Bülent Ecevit University. The XRD analysis was performed within a scanning range of 2θ = 5°-90°, with a step size of 0.02°-0.05°, and a measurement duration ranging between 15 and 60 minutes. Samples for XRD analysis were ground to <10 μm particle size and mounted using the powder diffraction method. Semi-quantitative mineral identification was performed using standard reference patterns and peak intensity comparisons.

Analytical Limitations: It should be noted that while quantitative mineral analysis using techniques such as Rietveld refinement would provide more precise modal abundances, such methods were not available for this study. The semi-quantitative approach employed here, combined with detailed petrographic analysis, provides reliable constraints on the major mineral phases and their relative abundances.

Table 1. Modal Analysis Results of the Examined Samples.

	Raw data							Normalized data		
Sample ID	Quartz (%)	Feldspar (%)	Rock Fragment (%)	Mica (%)	Amphibole (%)	Pyroxene (%)	Opaque Mineral (%)	Qm (%)	F (%)	Lt (%)
AR1	34.76	24.06	24.06	6.42	4.28	0.00	6.42	41.94	29.03	29.03
AR2	30.52	30.52	21.13	7.04	3.76	0.00	7.04	37.14	37.14	25.71
AR3	33.19	19.91	33.19	6.64	3.54	0.00	3.54	38.46	23.08	38.46
KO1	27.78	12.63	32.83	2.53	12.63	7.58	4.04	37.93	17.24	44.83
KO2	36.23	21.74	16.91	7.25	12.08	0.00	5.80	48.39	29.03	22.58
KO4	37.50	22.50	12.50	7.50	12.50	0.00	7.50	51.72	31.03	17.24
U1	31.79	20.23	20.23	14.45	8.67	0.00	4.62	44.00	28.00	28.00
U3	32.50	22.50	12.50	17.50	7.50	0.00	7.50	48.15	33.33	18.52
U4	29.57	24.19	24.19	13.44	4.30	0.00	4.30	37.93	31.03	31.03
U5	35.52	19.13	4.37	13.66	8.20	0.00	19.13	60.19	32.41	7.41
U6	25.59	21.65	33.46	9.84	4.72	0.00	4.72	31.71	26.83	41.46
KA1	35.71	26.19	26.19	7.14	2.38	0.00	2.38	40.54	29.73	29.73
KA2	30.09	20.83	34.72	6.94	3.70	0.00	3.70	35.14	24.32	40.54
KA4	33.68	23.32	4.15	23.32	7.77	0.00	7.77	55.08	38.14	6.78
Mean	**32.46**	**22.10**	**21.46**	**10.26**	**6.86**	**0.54**	**6.32**	**43.45**	**29.31**	**27.24**
Std. Dev.	**±3.44**	**±3.98**	**±10.37**	**±5.53**	**±3.58**	**±2.02**	**±4.06**	**±8.20**	**±5.47**	**±11.93**

3. Findings and Discussion

3.1. Petrographic characteristics

Systematic sampling was conducted in the Zonguldak Basin, specifically from the Kozlu, Armutçuk, Üzülmez, and Karadon regions (Figure 1). Modal analyses were completed on 14 samples, and the results are presented in Table 1. Statistical analysis of the modal data reveals mean values with standard deviations as follows: Quartz 32.46±3.44%, Feldspar 22.10±3.98%, Rock Fragments 21.46±10.37%, Mica 10.26±5.53%, Amphibole 6.86±3.58%, Pyroxene 0.54±2.02 and Opaque Mineral 6.32±4.06 (Table 1). The modal mineralogy of the rock samples collected from the Zonguldak Basin is summarized below.

The textural and compositional characteristics observed in the samples provide important insights into depositional processes and diagenetic history. The dominance of angular to sub-angular grain shapes suggests relatively short transport distances and rapid burial, consistent with proximal foreland basin settings. The preservation of unstable components such as feldspar and lithic fragments further supports this interpretation.

The textural characteristics of the samples from the Kozlu region indicate that they are medium-grained, with angular to sub-angular clastic fragments (sediment grains) cemented by a silica cement. The dominant texture of the rock is clastic and detrital. The mineral components within the texture consist of quartz, feldspar, mica, amphibole, and opaque minerals. The clastic fragments generally exhibit angular to sub-angular, subhedral (semi-euhedral) features (Figure 2). Petrographic mineral abbreviations follow [42].

The mineralogical composition of the samples collected from the Kozlu region is as follows: Quartz (35-40%): Occurs as anhedral, angular to sub-angular microcrystalline quartz clasts, with no observable signs of weathering on grain surfaces. Optically, they exhibit undulatory extinction and slight granulation (fracturing/cracking). The grain size distribution ranges from 0.25 to 0.55 mm. Feldspar-Plagioclase (Z) (20-25%): Alkali feldspars (orthoclase-microcline) are predominantly sericitized and partially kaolinized, while plagioclases remain unaltered, exhibiting polysynthetic twinning with a well-defined surface appearance. The general grain size distribution ranges from 0.33 to 0.6 mm, and they display subhedral (semi-euhedral), angular to sub-angular characteristics. Mica (Biotite, Muscovite) (5-10%): Composed of chloritized biotite (anhedral, pseudomorphic) and unaltered muscovite with a semi-rounded, platy appearance and fresh surface. The grain size ranges from 0.15 to 0.2 mm. Opaque Minerals (Magnetite-Hematite) (5-7%): Hematite occurs as fissure fillings with semi-angular to sub-rounded shapes, while magnetite is disseminated, exhibiting angular, semi-cubic, or subhedral forms. These opaque minerals are distributed among clasts or appear as opacifications along the outer margins and cleavage planes of biotites and amphiboles. The grain size varies between 0.1- and 0.55- mm. Amphibole (Hornblende) (10-15%): Mostly sub-angular, prismatic, and subhedral in shape. They are predominantly chloritized and exhibit opacification along their external margins. The grain size distribution ranges from 0.3 to 0.55 mm. Rock Fragments (Lithic Components) (15-20%): These fragments range in size from 0.33 to 0.66 mm and consist of angular to sub-angular, of igneous, metamorphic, and sedimentary origin (Table 1).

Feldspar grains exhibit angular to subangular morphologies. Notably, some K-feldspar fragments preserve subhedral crystal faces, suggesting relatively short transport distances and limited mechanical reworking prior to deposition.

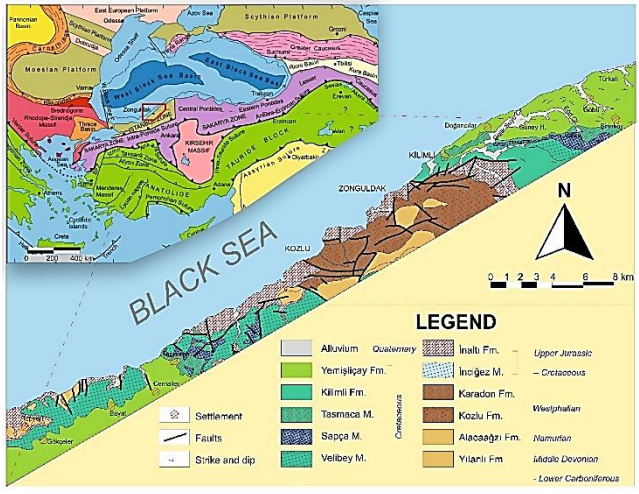

Figure 1. Geological map of the study area.

The preservation of subhedral crystal faces on detrital K-feldspar grains is significant as it indicates minimal transport distance from the source area and limited mechanical abrasion during transport. This textural characteristic suggests proximal depositional settings (e.g. alluvial fan or proximal fluvial environments) and relatively short residence time in the sedimentary system before burial. Such preservation is typically associated with rapid erosion and deposition in tectonically active settings, which is consistent with the sedimentary characteristics observed in the study area.

The textural characteristics of the samples collected from the Armutçuk region indicate that they are medium-grained, with angular to sub-angular clastic fragments (sediment grains) cemented by a silica cement. The dominant texture of the rock is clastic and detrital. The mineral components within the texture consist of quartz, feldspar, mica, amphibole, and opaque minerals (magnetite, hematite). The clastic fragments are generally angular to sub-angular and exhibit subhedral (semi-euhedral) characteristics (Figure 2).

The mineralogical composition of the samples collected from the Armutçuk region is as follows: Quartz (30-35%): Occurs as inter-crystalline fillings within the cement and as angular to sub-angular anhedral grains in the rock matrix. No signs of weathering are observed on the grain surfaces. Optically, they exhibit undulatory extinction, slight granulation (fracturing/cracking and grain size reduction), and local inclusions. The grain size distribution ranges from 0.25 to 0.83 mm. Feldspar - Plagioclase (Z) (20-25%): Alkali feldspars (orthoclase-microcline) are predominantly sericitized and partially kaolinized, displaying a perthitic texture. Plagioclases remain unaltered and exhibit polysynthetic twinning with a well-defined surface appearance. The grain size distribution ranges from 0.17 to 0.70 mm, and they display subhedral (semi-euhedral), angular to sub-angular characteristics. Rock Fragments (Lithic Components) (20-25%): These fragments range in size from 0.30 to 0.85 mm and are composed of subhedral, semi-rounded clasts of igneous, metamorphic, and sedimentary origin. Mica (Biotite, Muscovite) (5-7%): Composed of anhedral, sub-angular pseudomorphic chloritized biotite and unaltered muscovite, which has a semi-rounded, platy appearance with a fresh surface. The grain size varies between 0.25 and 0.83 mm. Opaque Minerals (Magnetite-Hematite) (5-7%): Found as pseudomorphic-relict grains (in biotite and hematite), occurring along the external surfaces, grain boundaries, or cleavage planes as fissure fillings. Magnetite is disseminated and appears as subhedral, angular to sub-angular, cubic grains. The average grain size distribution ranges from 0.17 to 0.58 mm. Amphibole (Hornblende) (3-5%): Mostly sub-angular, prismatic, and subhedral, with chloritized pseudomorphic characteristics. The grains are abraded and fragmented, often appearing as relict subhedral grains. The grain size distribution ranges from 0.35 to 0.70 mm (Table 1).

The textural characteristics of the samples collected from the Üzülmez region indicate grain sizes ranging from coarse silt to coarse sand (0.04–0.50 mm), predominantly fine- to medium-grained, with angular to sub-angular clastic fragments. The dominant texture of the rock is clastic and detrital. The mineral components within the texture consist of quartz, feldspar, mica, amphibole, and opaque minerals. The clastic fragments are generally angular to sub-angular and exhibit subhedral (semi-euhedral) characteristics (Figure 2).

The mineralogical composition of the samples collected from the Üzülmez region is as follows: Quartz (25-30%): Occurs as anhedral, angular to sub-angular grains, displaying a slightly oriented arrangement consistent with lamination. No signs of weathering are observed on the grain surfaces. Optically, they exhibit undulatory extinction and slight granulation (fracturing/cracking). The grain size distribution ranges from 0.17 to 0.6 mm. Feldspar-Plagioclase (Z) (20-25%): Alkali feldspars (orthoclase-microcline) are predominantly sericitized and kaolinized, exhibiting perthitic texture, while plagioclases remain unaltered and display polysynthetic twinning. The general grain size distribution ranges from 0.25 to 0.6 mm, with subhedral (semi-euhedral), angular to sub-angular characteristics. Mica (Biotite, Muscovite) (10-15%): Consists of chloritized biotite, which appears anhedral and pseudomorphic, with opacification along its external edges, and unaltered muscovite, which has a platy appearance with a fresh surface. The grain size varies between 0.25- and 0.70- mm. Opaque Minerals (Magnetite-Hematite) (3-5%): Hematite occurs as iron oxide-rich intergranular layers and as semi-angular to sub-rounded grains, whereas magnetite is disseminated and appears as angular grains. The grain size ranges from 0.25 to 0.5 mm. Rock Fragments (Lithic Components) (20-25%): These fragments range in size from 0.45 to 0.7 mm and consist of subhedral siliceous and carbonate rock fragments. Amphibole (Hornblende) (3-5%): Mostly sub-angular, anhedral, and predominantly chloritized. The grain size distribution ranges from 0.25 to 0.6 mm. Carbonate Minerals (Calcite) (2-3%): Occurs as subhedral, rhombohedral grains, locally distributed between quartz and feldspar grains. The grain size distribution ranges from 0.32 to 0.83 mm (Table 1). The textural characteristics of the samples collected from the Karadon region indicate that they are medium-grained, with clastic fragments (sediment grains) cemented by a silica cement. The dominant texture of the rock is clastic and detrital. The mineral components within the texture consist of quartz, feldspar, mica, amphibole, and opaque minerals. The clastic fragments are generally angular to sub-angular and exhibit subhedral (semi-euhedral) characteristics (Figure 2). The mineralogical composition of the samples collected from the Karadon region is as follows: Quartz (35-40%): Present as inter-crystalline fillings within the cement and as angular to sub-angular anhedral grains in the rock matrix. No signs of weathering are observed on grain surfaces. Optically, they exhibit undulatory extinction and slight granulation (fracturing/cracking and grain size reduction).

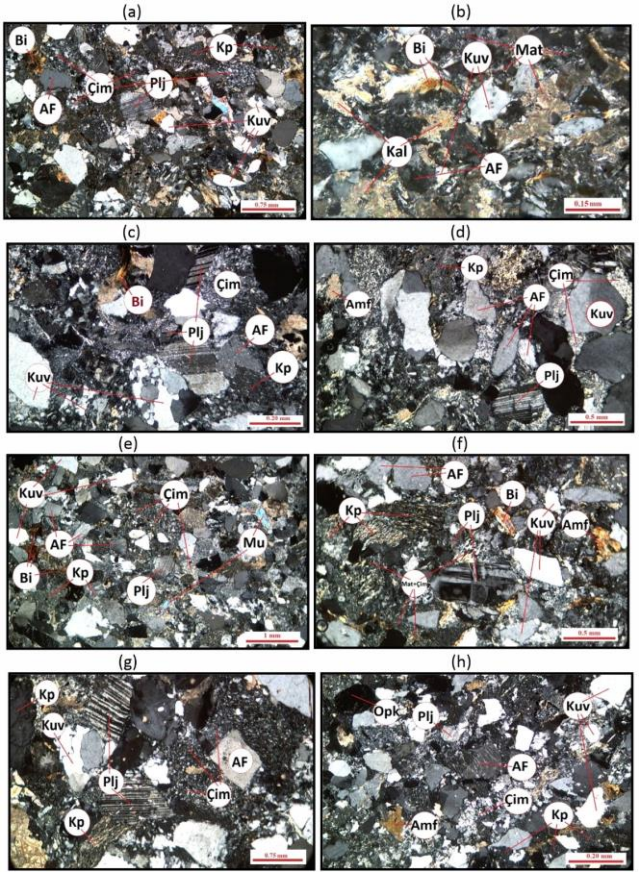

Figure 2. (a-b) Medium-grained texture of sandstone from the Kozlu Region (ppl, Qz: quartz, Afs: alkali feldspar, Bt: biotite, Rf: rock fragment, Pl: plagioclase, Cmt: cement, Cal: calcite, Mtx: matrix). (c-d) Medium-grained texture of sandstone from the Karadon region (ppl, Qz: quartz, Afs: alkali feldspar, Rf: rock fragment, Pl: plagioclase, Opq: opaque mineral, Cmt: cement). (e-f) Fine to medium-grained texture of sandstone from the Üzülmez region (ppl, Qz: quartz, Rf: rock fragment, Bt: biotite, Pl: plagioclase, Ms: muscovite, Cmt: cement). (g-h) Medium-grained texture of sandstone from the Armutçuk Region (ppl, Qz: quartz, Afs: alkali feldspar, Rf: rock fragment, Pl: plagioclase, Opq: opaque mineral, Amp: amphibole, Cmt: cement) [42].

The grain size distribution ranges from 0.25 to 0.75 mm. Feldspar-Plagioclase (Z) (25-30%): Alkali feldspars (orthoclase-microcline) are predominantly sericitized and partially kaolinized, while plagioclases remain unaltered and display polysynthetic twinning with a well-defined surface appearance.

The general grain size distribution ranges from 0.25 to 0.5 mm, with subhedral (semi-euhedral), angular to sub-angular characteristics. Rock Fragments (Lithic Components) (25-30%): These fragments range in size from 0.415 to 0.85 mm and consist of subhedral, semi-rounded clasts of igneous, metamorphic, and sedimentary origin. Mica (Biotite, Muscovite) (5-10%): Consists of anhedral, sub-angular pseudomorphic chloritized biotite and unaltered muscovite, which has a semi-rounded, platy appearance with a fresh surface. The grain size varies between 0.25- and 0.67- mm. Opaque Minerals (Magnetite-Hematite) (2-3%): Hematite occurs as anhedral fissure fillings, while magnetite is disseminated and appears as angular, semi-cubic to subhedral cubic grains. The grain size distribution ranges from 0.25 to 0.42 mm. Amphibole (Hornblende) (2-3%): Mostly sub-angular, prismatic, and subhedral, with chloritized pseudomorphic characteristics. The grains are often fragmented, appearing as relict subhedral grains. The grain size distribution ranges from 0.3 to 0.6 mm. Carbonate (Calcite) (3-5%): Occurs as subhedral, semi-angular, rhombohedral cleaved grains, either as secondary carbonate fillings between grains or as transported and fragmented clastic particles. The grain size distribution ranges from 0.33 to 0.65 mm (Table 1).

When the analyzed samples are plotted on the Quartz-Feldspar-Rock Fragment triangular diagram [9], it is observed that they predominantly fall within the Feldspathic Litharenite, Arkose, and Lithic Arkose fields (Figure 3). This indicates that the samples were transported in high-energy environments. Notably, a significant proportion of the samples contain 50-75% lithic fragments, highlighting their abundance in rock-derived clasts. Such rock types typically contain a high proportion of lithic fragments and are generally associated with tectonically active regions. This distribution suggests that the sedimentary rocks were formed from material sourced from tectonically active environments [10].

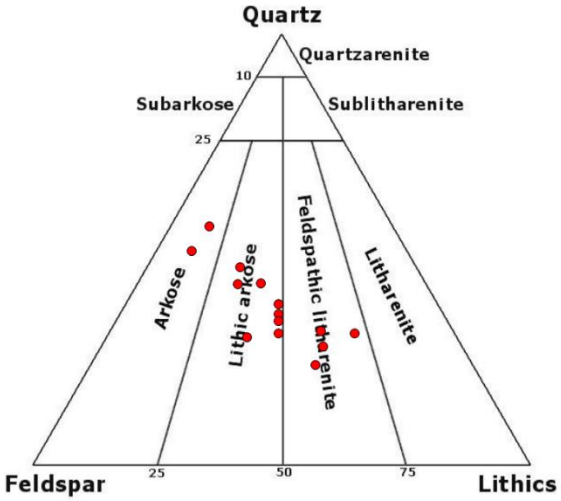

Figure 3. Quartz-feldspar-rock fragment ternary diagram [9].

3.2. Tectono-sedimentary implications

The mineralogical composition and grain size distribution of the sandstone samples from the Zonguldak Basin were analyzed using both petrographic examination and X-Ray Diffraction (XRD) techniques. The results provide critical insights into the provenance, depositional environment, and post-depositional processes that affected the studied units. Modal analysis reveals quartz-dominated framework grains with significant feldspar (plagioclase and K-feldspar, averaging 25-30%) and lithic fragments. QFL ternary diagrams [11] show samples plotting predominantly in dissected arc and transitional arc fields (Figure 6), consistent with the observed mineralogy: (1) high feldspar content indicating plutonic arc basement contribution, (2) amphibole presence derived from intermediate-felsic intrusions, and (3) volcanic lithic fragments with quartz-feldspar phenocrysts representing both volcanic cover and comagmatic plutons. Dissected arcs represent mature magmatic systems where erosion and uplift expose deeper plutonic levels [10], explaining the elevated feldspar/lithic ratios and plutonic mineral assemblages. The fresh angular feldspar grains and limited alteration indicate rapid erosion, short transport, and/or rapid burial in a tectonically active setting. This provenance signature is diagnostic of an active continental margin with subduction-related arc magmatism undergoing syn-depositional dissection [10, 12].

The presence of significant lithic fragments could also indicate contributions from recycled sedimentary sources or extensional settings where basement blocks are rapidly exhumed [11, 13]. However, the specific combination of angular feldspar grains, volcanic lithic fragments, and limited chemical alteration strongly favours the active margin interpretation over passive margin or cratonic sources. This is because: (1) volcanic lithics indicate syn-depositional arc magmatism rather than limited intraplate volcanism [10], (2) fresh angular feldspars suggest first-cycle derivation with minimal weathering unlike the mature assemblages typical of passive margins [14, 15], (3) framework compositions plot in the magmatic arc field on provenance diagrams (Figure 6) consistent with active continental margin settings [11, 16], and (4) the absence of sedimentary lithic fragments excludes recycled orogen sources [17]. These characteristics collectively distinguish active margin settings from extensional or cratonic alternatives.

XRD analyses complement petrographic data, confirming the presence of quartz, feldspar, clay minerals (including illite and muscovite), and minor calcite. The relatively sharp diffraction peaks of quartz and feldspar indicate well-crystallized detrital grains, while the broader peaks associated with clay minerals imply diagenetic transformation processes during burial [18, 19]. The occurrence of calcite suggests limited carbonate cementation, likely derived from groundwater during early diagenesis.

Diagenetic Processes: The presence of illite and muscovite as identified by XRD analysis warrants detailed discussion regarding their origin. While muscovite likely represents detrital mica derived from metamorphic sources or igneous sources, illite formation can occur through diagenetic alteration of detrital feldspars and other aluminosilicate minerals during burial. The broad XRD peaks associated with clay minerals suggest lower crystallinity typical of diagenetic rather than detrital origin, indicating burial temperatures in the range of 60-120 °C [19]. This temperature range is consistent with the moderate burial depths expected in foreland basin settings and supports the interpretation of post-depositional alteration processes.

The partial kaolinization of feldspars observed in thin sections may represent either surficial weathering in the source area or early diagenetic alteration in the depositional environment. The limited extent of this alteration suggests relatively arid source area conditions or rapid burial that prevented extensive chemical weathering.

Folk's rock classification method is widely utilized, particularly for sandstones, as it defines rock types based on the relative proportions of feldspar, quartz, and lithic fragments [9]. Upon examination of the tabular data, it is observed that the majority of the samples fall within the Feldspathic Litharenite group, while the remaining samples are distributed in the Lithic Arkose and Arkose fields (Table 2).

Grain size analysis shows that the sandstones range from fine- to medium-grained, with occasional coarse fractions. This texture suggests deposition under fluctuating energy conditions, possibly in fluvial-deltaic systems where episodic high-energy flows transported sediments across short distances. While finer grains are indicative of deposition in lower energy settings such as floodplains or delta fronts, the presence of angular lithic fragments points to a relatively immature sedimentary system with limited abrasion [20]..

Table 2. Petrographic characteristics and compositional classification of sandstone samples.

Sample ID	Mean Grain Size (mm)	Grain Size Classification (Folk, 1974; Tucker, 2001)	Folk Compositional Classification (Folk, 1974)
AR1	0.51	Coarse sand	Feldspathic Litharenite
AR2	0.71	Coarse sand	Lithic Arkose
AR3	0.53	Coarse sand	Feldspathic Litharenite
KO1	0.32	Medium sand	Feldspathic Litharenite
KO2	0.38	Medium sand	Lithic Arkose
KO4	0.51	Coarse sand	Lithic Arkose
U1	0.18	Fine sand	Feldspathic Litharenite
U3	0.10	Very fine sand	Lithic Arkose
U4	0.50	Medium-Coarse sand	Feldspathic Litharenite
U5	0.04	Coarse silt	Arkose
U6	0.50	Medium-Coarse sand	Feldspathic Litharenite
KA1	0.50	Medium-Coarse sand	Feldspathic Litharenite
KA2	0.53	Coarse sand	Feldspathic Litharenite
KA4	0.04	Coarse silt	Arkose

Moreover, the combination of angular lithic fragments, abundant feldspar, and varied grain size supports the interpretation of a tectonically active basin margin, where active uplift and erosion dominate sediment supply. Such characteristics are typical of foreland basins or arc-adjacent depocenters [21]. These findings are consistent with regional tectonic reconstructions that suggest the Zonguldak Basin was influenced by the closure of the Intrapontide Ocean and subsequent collisional events during the Paleozoic–Mesozoic transition [22].

Taken together, the mineralogical and textural characteristics of the studied sandstones support a depositional setting marked by active tectonism, rapid erosion, and short transport, highlighting the role of orogenic processes in shaping the sedimentological character of the Zonguldak Basin.

3.3. X-Ray diffraction (XRD) results and integration with petrography

To partially investigate the mineralogical composition and assess potential diagenetic alterations, X-Ray Diffraction (XRD) analyses were performed on four representative sandstone samples: AR-1 (Armutçuk), KA-1 (Karadon), KO-2 (Kozlu), and U-4 (Üzülmez). While increasing the number of XRD analyses would enhance statistical reliability, the four samples analyzed provide representative coverage of the major formations and lithofacies present in the study area. Additional XRD analyses were not feasible due to practical constraints including sample availability and analytical costs

The XRD diffractograms (Figures 4 and 5) reveal the presence of major mineral phases consistent with the petrographic findings. Peak identification and d-spacing assignments are as follows:

Detailed Peak Analysis:

Quartz: Primary peaks at d = 3.31-3.33 Å (101 reflection), 4.21-4.24 Å (100 reflection), and 1.82 Å (110 reflection).

Feldspar minerals: Characteristic peaks at d = 4.20-4.40 Å corresponding to (100) and (110) planar reflections of both plagioclase and alkali feldspar.

Clay minerals (illite/muscovite): Diagnostic peaks at d = 3.16-3.17 Å (002 reflection) and 10.0 Å (001 reflection).

Calcite: Minor peaks at d = 2.43-2.44 Å (202 reflection) and 3.04 Å (104 reflection)

The sharp, well-defined peaks for quartz and feldspar indicate high crystallinity typical of detrital grains derived from igneous and metamorphic sources. In contrast, the broader, lower-intensity peaks for clay minerals suggest diagenetic origin and lower crystallinity, consistent with formation during burial processes rather than inheritance from source rocks [23, 24].

Correlation with Petrographic Data: The XRD results corroborate the modal analysis data obtained via petrography (Table 1) for the four analyzed samples. The high relative intensities of quartz and feldspar peaks are consistent with the significant presence of these minerals observed under the microscope in these specific samples. The detection of illite and muscovite by XRD confirms the presence of mica observed petrographically (Table 1). The minor calcite peak corresponds to the sparse carbonate grains (calcite) noted in thin sections, particularly in samples from the Üzülmez and Karadon regions (e.g. Figure 2f, h).

Crystallinity: Analysis of peak shapes provides further insights for the analyzed samples. The relatively sharp diffraction peaks for quartz and feldspar indicate well-crystallized detrital grains, supporting their primary origin from stable source rocks (likely felsic igneous or high-grade metamorphic terrains, as inferred from lithic fragment compositions and consistent with provenance interpretations in Section 3.4. [10]).

Quantitative Considerations and Sample Limitations: While XRD provides qualitative and semi-quantitative information, precise quantification of mineral proportions requires specialized techniques (e.g. Rietveld refinement) which were not applied in this study. Importantly, XRD analysis was limited to four bulk powder samples due to practical constraints, and no oriented clay-fraction preparations, glycolation, or thermal treatments were performed. Therefore, the XRD results offer only a preliminary mineralogical characterization of these four samples and cannot be extrapolated to basin-scale interpretations. The relative peak intensities are consistent with the general mineralogical trends identified in the petrographic analysis (Table 1) for these specific samples only. Integrating these findings with the broader petrographic dataset (n = 14) provides complementary information, but petrographic observations remain the primary basis for basin-wide sedimentary interpretations.

This combined petrographic and XRD approach confirms the presence and dominance of quartz and feldspar and the occurrence of lithic fragments (validated petrographically) in the analyzed samples. These mineralogical constraints complement the subsequent tectonic provenance analysis presented in section 3.4.

3.4. Tectonic Regime and Rock Provenance

The Zonguldak Basin is one of Turkey's most significant coal-bearing regions, located along the southern coast of the Black Sea [25, 26]. This area has been subjected to various tectonic regimes since the Paleozoic and Mesozoic periods [27, 28]. Considering the coalification processes during the Carboniferous period and the impact of an active tectonic regime since the Cretaceous [22, 29], the region serves as an example of orogenic processes and active continental margin evolution. The quartz content (32.46%) is at a moderate level, indicating that the basin is in a transition process from a passive to an active continental margin and

may also be associated with active tectonic environments [7, 13]. The high feldspar content (22.10%) suggests that the rocks originated from young continental crust, influenced by active continental margins or orogenic processes [30, 31]. The presence of rock fragments and volcanic lithics (21.46%) supports the existence of Cretaceous and post-Cretaceous volcanic activity in the Zonguldak Basin [32, 33].

The Qm-F-Lt ternary diagram provides critical insights into the tectonic setting of the source area for the studied sandstones (Figure 6) [10, 11]. The 14 samples display a coherent compositional trend, with the majority plotting within the Dissected Arc field and subordinate samples falling in the Transitional Arc field. This distribution pattern indicates derivation from a magmatic arc terrane that has undergone significant tectonic uplift and erosional unroofing.

The majority of samples plotting in the Dissected Arc field suggests that the source area was characterized by deeply eroded volcanic-plutonic complexes, where extensive denudation has exposed intermediate to felsic plutonic rocks (granitoids, tonalites, granodiorites) beneath the volcanic cover [13]. This interpretation is supported by the relatively high feldspar content and the presence of diverse lithic fragments, which are typical of mature arc systems subjected to prolonged erosion and tectonic exhumation [7, 30]. Additionally, several samples plotting in the Transitional Arc field indicate a mixed provenance involving both volcanic and plutonic sources, suggesting that the source terrane retained partial volcanic cover during sedimentation and reflecting intermediate stages of arc dissection [17]. This transitional character may also imply temporal or spatial variations in the degree of arc maturity and erosional depth within the source region [34], indicating a complex and evolving magmatic arc system that supplied sediment to the basin.

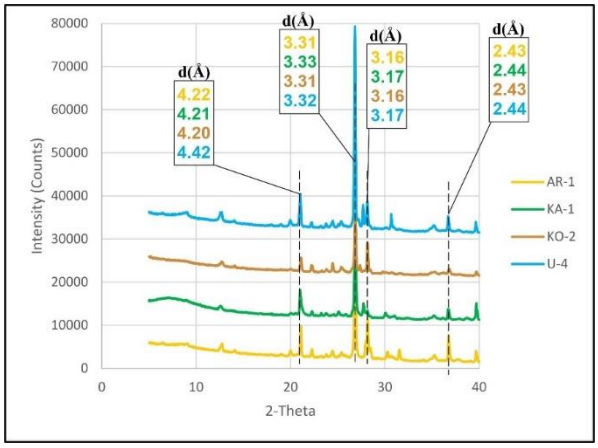

Figure 4. D(Å) angles based on x-ray diffraction (XRD) analysis results.

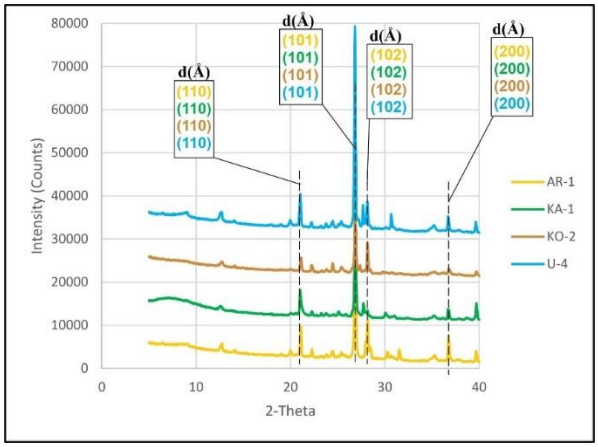

Figure 5. X-ray diffraction (xrd) analysis result graph based on miller indices.

Independent detrital zircon U–Pb data from the Upper Carboniferous Kozlu Sandstone (Kozlu, Zonguldak) show ages between 2371–315 Ma, dominated by a late Neoproterozoic–early Cambrian population (740–495 Ma; ~74%), with subordinate Ordovician–Carboniferous grains (485–315 Ma; ~12%) and minor Paleoproterozoic ages." [35].

When the tectonic setting of the study area is evaluated in conjunction with the global movements of the continents and the source rock and provenance analyses derived from the examined sandstones, it is suggested that the source rock evolved from a subduction zone developed over Avalonia (Figure 7a, 7b) to an erosion region along the advancing thrust zone (Figure 7c). Therefore, the granitic masses shown in red in Figure 7C, which are rich in feldspar, one of the primary components of the sandstones, emerge as the main source of the sedimentary material. This is consistent with the provenance analysis of the sandstones.

Based on the provenance analysis, it is observed that the examined sandstone samples are located within the Transitional Arc and Dissected Arc regions. The Transitional Arc environment indicates a provenance type associated with the magmatic arc system, where rock fragments (lithics) still play a significant role. This supports the hypothesis that the granitic masses eroded from Avalonia could have weathered into the source rock for the sandstones. [35].

On the other hand, the samples from the Dissected Arc environment represent more eroded and weathered magmatic rocks. This suggests that the source has been exposed to chemical and physical weathering for a longer period, and that the sandstones originated from metamorphic and granitic rocks. In particular, the high feldspar content demonstrates that the magmatic rocks in the source region have weathered and contributed to the sedimentation process.

Moreover, the formation of the economically significant coal seams in the Zonguldak Basin is considered a result of the development of swamp environments during the closure of the Rheic Ocean. During the Carboniferous period, large amounts of organic material accumulated under the swamp conditions in the region and gradually underwent coalification [36]. Thus, with the closure of the Rheic Ocean, the active tectonic processes in the region shaped the depositional environments of the basin and created favourable conditions for coal formation.

In the later stages of tectonic evolution, the collision of the Hun Continent, thought to have included the Kırşehir Massif and Konya regions, with Laurentia + Avalonia resulted in the Variscan orogeny (Figure 7d). During the Cimmerian orogeny, Gondwana also joined this collision, leading to the formation of Pangea [35].

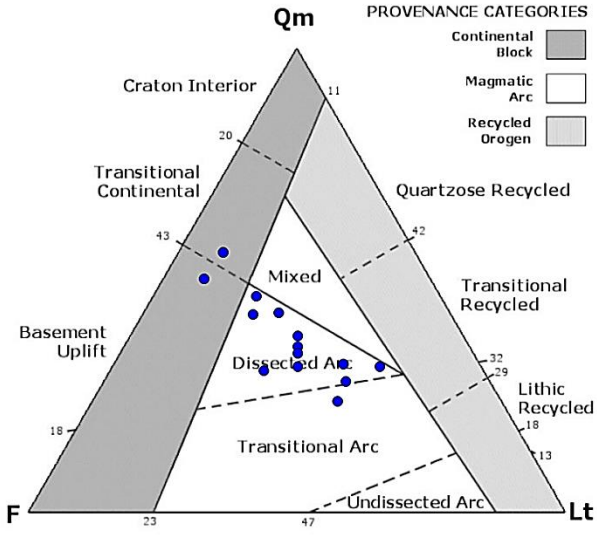

Figure 6. Quartz, feldspar, and rock fragment tectonic ternary diagram [10]

Both the Variscan orogeny and the Cimmerian orogeny caused the tectonic positions of the sandstones examined in this study to align with their present-day positions (Figure 7e). Temporal Evolution and Source Area Development: The paleotectonic reconstruction (Figure 7) suggests that the source rock evolved from a subduction zone developed over Avalonia to an erosion region along an advancing thrust zone [37, 43-45]. The granitic masses rich in feldspar emerge as the main source of sedimentary material, consistent with the observed provenance signatures. This interpretation aligns with broader models of Variscan orogenic evolution in the region [37].

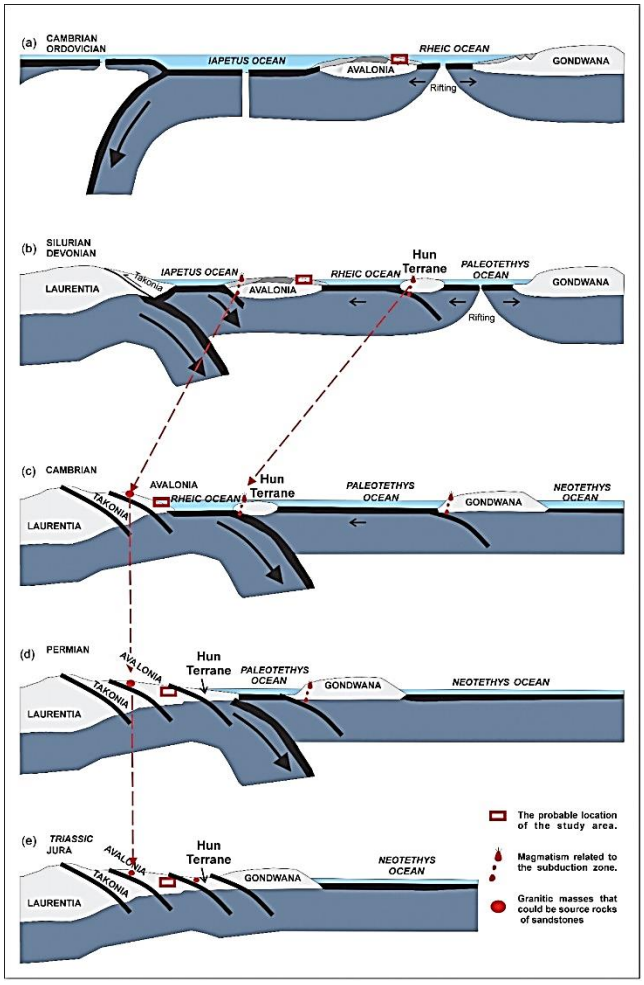

Figure 7. Global plate movements and the position of the study area during the Paleozoic era (a) Cambrian – Ordovician: opening of the Rheic ocean, and subduction of the Iapetus ocean. (b) Silurian – Devonian: separation of the Hun Continent from Gondwana, and the beginning of the Paleotethys opening. (c) Carboniferous: completion of the closure of the Rheic ocean, the start of the closure of the Paleotethys, and the birth of the Neotethys. (d) Permian: collision of the Hun Continent with Laurentia – Avalonia. (e) Triassic – Jurassic: collision of Gondwana with other continents during the Cimmerian Orogeny, leading to the formation of Pangea. (the figure is adapted from [37,43-45]).

4. Conclusion

The mineralogical and petrographic properties of sandstone samples collected from the Zonguldak Basin have been examined in detail through modal analysis, petrographic microscopy, and XRD techniques. The majority of the samples are classified as Feldspathic Litharenite, Arkose, and Lithic Arkose, indicating that they were derived from multi-source terranes and deposited in dynamic, high-energy environments. The high abundance of lithic fragments and feldspar components reflects the proximity of tectonically active orogenic sources, such as magmatic arcs and uplifted continental blocks [10, 38].

X-Ray Diffraction (XRD) results confirmed the presence of quartz, feldspar, clay minerals, and calcite as major mineral phases. While the XRD analysis was limited to four samples due to practical constraints, these samples provide representative coverage of the major formations and show consistent mineralogical trends that support the provenance interpretations. The mineral assemblage suggests that, in addition to detrital input from granitic and metamorphic sources, the rocks also underwent post-depositional diagenetic processes, such as feldspar alteration and clay formation, indicative of burial or early compaction stages [19].

The arc-related signature observed in the samples is consistent with derivation from magmatic arc complexes associated with subduction zone settings [39, 40]. In the regional context of the study area, this provenance pattern likely reflects erosion of the Sakarya Zone to the north, which hosts extensive Late Cretaceous to Paleocene magmatic rocks related to the northward subduction and subsequent closure of the Neotethys Ocean [22, 28, 32]. The tectonic uplift and unroofing of these arc complexes would have supplied abundant feldspathic and lithic-rich detritus to the adjacent sedimentary basin [33, 41].

The proximity of some samples to the Continental Block field suggests a subordinate contribution from continental basement rocks, possibly representing input from uplifted crustal blocks or back-arc regions where arc-derived material mixed with older continental sources [31, 40].

In conclusion, this study demonstrates the value of integrated petrographic and mineralogical analysis for understanding basin evolution in active tectonic settings. The results provide a foundation for future studies aimed at understanding the broader implications of Variscan and Alpine orogenic processes in the development of Paleozoic-Mesozoic sedimentary basins in the eastern Mediterranean region.

Acknowledgement

We would like to express our gratitude to the Laboratory of the Faculty of Mining Engineering at Istanbul Technical University for their support in the preparation of thin sections. We also extend our sincere thanks to the ARTMER Laboratory at Zonguldak Bülent Ecevit University for conducting the XRD analyses. The authors acknowledge that while additional XRD analyses would strengthen the statistical foundation of this study, the four samples analyzed provide representative insights into the mineralogical characteristics of the Zonguldak Basin sandstones.

Funding

The authors did not receive support from any organization for the submitted work.

Conflict of interest

The authors have no conflicts of interest to declare that are relevant to the content of this article.

Author contributions

Zikrullah Samet Güloğlu: Methodology, Conceptualization, Writing - original draft, Writing - review & editing. Çağrı Aldı: Methodology, Conceptualization, Writing - original draft. Halil Bölük: Conceptualization, Writing - review & editing. Olgay Yaralı: Review & editing.

References

[1] Gök, M. Ş., 1970. Kuzey Anadolu Taşkömür Havzası (Tektonik Yapısı). Türkiye Jeoloji Bülteni, 13(1), 120-145.

[2] Yalçın, M.N., İnan, S., Gülbin, G., Mann, U., Schaefer, R.G., 2002. "Carboniferous coals of the Zonguldak basin (northwest Turkey): Implications for coalbed methane potential." American Association of Petroleum Geologists Bulletin, 86(7), 1305-1328.

[3] Aydın, M., Yalçın, M. N., Mann, U., 2011. Carboniferous coal measures of the Zonguldak Basin, NW Turkey: Implications for coalbed methane potential. International Journal of Coal Geology, 85(3), 168-179.

[4] Tuncalı, E., 1996. Stratigraphy and depositional environments of the Carboniferous coal-bearing sequences in the Zonguldak region. Turkish Journal of Earth Sciences, 5(2), 89-102.

[5] Göncüoğlu, M.C., Kozlu, H., 2000. "Early Paleozoic evolution of the NW Gondwanaland: Data from southern Turkey and surrounding regions." Gondwana Research, 3, 315-324.

[6] Maden Tetkik ve Arama Genel Müdürlüğü (MTA) 2023. Kozlu Kömür Sahasında (Zonguldak Havzası, KB Türkiye) Açılan İki Derin Araştırma Kuyusunda Geç Karbonifer Yaşlı İstiflerin İncelenmesi. Maden Tetkik ve Arama Dergisi

[7] Dickinson, W.R., 1985, Interpreting provenance relations from detrital modes of sandstones, in Zuffa, G.G., ed., Provenance of Arenites: Dordrecht, Reidel Publishing Company, p. 333-361.

[8]Ingersoll, R. V., Bullard, T. F., Ford, R. L., Grimm, J. P., Pickle, J. D., & Sares, S. W. (1984). The effect of grain size on detrital modes: A test of the Gazzi-Dickinson point-counting method. Journal of Sedimentary Petrology, 54(1), 103-116. https://doi.org/10.1306/212F83B9-2B24-11D7-8648000102C1865D

[9] Folk, R. L., 1974. Petrology of sedimentary rocks. Hemphill Publishing Company.

[10] Dickinson, W. R., Suczek, C. A., 1979. Plate tectonics and sandstone compositions. AAPG Bulletin, 63(12), 2164-2182.

[11] Dickinson, W.R., Beard, L.S., Brakenridge, G.R., Erjavec, J.L., Ferguson, R.C., Inman, K.F., Knepp, R.A., Lindberg, F.A., and Ryberg, P.T., 1983, Provenance of North American Phanerozoic sandstones in relation to tectonic setting: Geological Society of America Bulletin, v. 94, p. 222-235.

[12] Boggs, S., 2009. Petrology of Sedimentary Rocks. Cambridge University Press.

[13] Ingersoll, R.V., and Suczek, C.A., 1979, Petrology and provenance of Neogene sand from Nicobar and Bengal fans, DSDP sites 211 and 218: Journal of Sedimentary Petrology, v. 49, p. 1217-1228.

[14] Johnsson, M.J., Stallard, R.F., Meade, R.H., 1991. First-cycle quartz arenites in the Orinoco River basin, Venezuela and Colombia. Journal of Geology 99, 263-274.

[15] Garzanti, E., 2019. Petrographic classification of sand and sandstone. Earth-Science Reviews 192, 545-563.

[16] Garzanti, E., 2016. From static to dynamic provenance analysis—Sedimentary petrology upgraded. Sedimentary Geology 336, 3-13.

[17] Ingersoll, R.V., 1983, Petrofacies and provenance of late Mesozoic forearc basin, northern and central California: American Association of Petroleum Geologists Bulletin, v. 67, p. 1125-1142.

[18] Moore, D. M., Reynolds, R. C., 1997. X-Ray Diffraction and the Identification and Analysis of Clay Minerals. Oxford University Press.

[19] Worden, R. H., Morad, S., 2003. Clay minerals in sandstones: controls on formation, distribution and evolution. IAS Special Publication, 34, 3–41.

[20] Tucker, M. E., 2001. Sedimentary Petrology: An Introduction to the Origin of Sedimentary Rocks. Wiley-Blackwell.

[21] Ingersoll, R. V., 1988. Tectonics of sedimentary basins. Geological Society of America Bulletin, 100(11), 1704–1719.

[22] Okay, A. I., Tüysüz, O., 1999. Tethyan evolution of Turkey: A plate tectonic approach. Tectonophysics, 271(1-2), 1-27.

[23] Warr, L.N., Ferreiro Mählmann, R., 2015. Recommendations for Kübler Index standardization. Clay Minerals 50, 283-286.

[24] Katz, D.A., Rendon, V.R., Schroeder, L.W., Rettke, R., Schmitt, D.R., 2018. A new collection of clay mineral 'Crystallinity' Index Standards and revised guidelines for the calibration of Kübler and Árkai indices. Clay Minerals 53, 339-350.

[25] Okay, A.I., Şengör, A.M.C., and Görür, N., 1994, Kinematic history of the opening of the Black Sea and its effect on the surrounding regions: Geology, v. 22, p. 267-270.

[26] Kerey, İ.E., Meriç, E., Tunoğlu, C., Kelling, G., Brenner, R.L., and Doğan, A.U., 2004, Black Sea-Marmara Sea Quaternary connections: new data from the Bosphorus, Istanbul, Turkey: Palaeogeography, Palaeoclimatology, Palaeoecology, v. 204, p. 277-295.

[27] Görür, N., Oktay, F.Y., Seymen, İ., and Şengör, A.M.C., 1997, Paleozoic evolution of the Zonguldak region, in Ağa, Ö.A., Taner, G., and Gürdal, G., eds., Geology of the Black Sea Region: Ankara, MTA General Directorate, p. 3-12.

[28] Yılmaz, Y., Tüysüz, O., Yiğitbaş, E., Genç, Ş.C., and Şengör, A.M.C., 1997, Geology and tectonic evolution of the Pontides, in Robinson, A.G., ed., Regional and Petroleum Geology of the Black Sea and Surrounding Region: American Association of Petroleum Geologists Memoir 68, p. 183-226.

[29] Tüysüz, O., 1999, Geology of the Cretaceous sedimentary basins of the Western Pontides: Geological Journal, v. 34, p. 75-93.

[30] Marsaglia, K.M., and Ingersoll, R.V., 1992, Compositional trends in arc-related, deep-marine sand and sandstone: a reassessment of magmatic-arc provenance: Geological Society of America Bulletin, v. 104, p. 1637-1649.

[31] Garzanti, E., Andò, S., and Vezzoli, G., 2007, Settling equivalence of detrital minerals and grain-size dependence of sediment composition: Earth and Planetary Science Letters, v. 273, p. 138-151.

[32] Topuz, G., Altherr, R., Schwarz, W.H., Siebel, W., Satır, M., and Dokuz, A., 2005, Post-collisional plutonism with adakite-like signatures: the Eocene Saraycık granodiorite (Eastern Pontides, Turkey): Contributions to Mineralogy and Petrology, v. 150, p. 441-455.

[33] Ustaömer, P.A., and Robertson, A.H.F., 2010, Late Palaeozoic–Early Cenozoic tectonic development of the Eastern Pontides (Artvin area), Turkey: stages of closure of Tethys along the southern margin of Eurasia: Geological Society, London, Special Publications, v. 340, p. 281-327.

[34] Critelli, S., and Ingersoll, R.V., 1994, Sandstone petrology and provenance of the Siwalik Group (northwestern Pakistan and western-southeastern Nepal): Journal of Sedimentary Research, v. A64, p. 815-823.

[35] Akdoğan, R., Hu, X., Okay, A. I., Topuz, G., & Xue, W. (2021). Provenance of the Paleozoic to Mesozoic siliciclastic rocks of the Istanbul Zone constrains the timing of the Rheic Ocean closure in the Eastern Mediterranean region. Tectonics, 40, e2021TC006824. https://doi.org/10.1029/2021TC006824

[36] Şengör, A. M. C., & Yılmaz, Y. (1981). Tethyan evolution of

Turkey: A plate tectonic approach. Tectonophysics, 75(3–4), 181–241. https://doi.org/10.1016/0040-1951(81)90275-4

[37] Stampfli, G. M., Borel, G. D., 2002. A plate tectonic model for the Paleozoic and Mesozoic constrained by dynamic plate boundaries and restored synthetic oceanic isochrons. Earth and Planetary Science Letters, 196(1-2), 17-33. DOI: https://doi.org/10.1016/S0012-821X(01)00588-X

[38] Blatt, H., Middleton, G., Murray, R., 1980. Origin of sedimentary rocks. Prentice-Hall.

[39] Cawood, P.A., Hawkesworth, C.J., and Dhuime, B., 2012, Detrital zircon record and tectonic setting: Geology, v. 40, p. 875-878.

[40] Dickinson, W.R., and Gehrels, G.E., 2009, Use of U-Pb ages of detrital zircons to infer maximum depositional ages of strata: A test against a Colorado Plateau Mesozoic database: Earth and Planetary Science Letters, v. 288, p. 115-125.

[41] Okay, A.I., Sunal, G., Sherlock, S., Altıner, D., Tüysüz, O., Kylander-Clark, A.R.C., and Aygül, M., 2013, Early Cretaceous sedimentation and orogeny on the active margin of Eurasia: Southern Central Pontides, Turkey: Tectonics, v. 32, p. 1247-1271.

[42] Warr, L.N., 2021. IMA–CNMNC approved mineral symbols. Mineralogical Magazine 85, 291–320. https://doi.org/10.1180/mgm.2021.43

[43] Scotese, C. R., 2001. Atlas of Earth History, Volume 1, Paleogeography. PALEOMAP Project. Retrieved from https://www.earthbyte.org/paleomap-paleoatlas-for-gplates/

[44] Domeier, M., Torsvik, T. H., 2014. Plate tectonics in the late Paleozoic. Geoscience Frontiers, 5(3), 303-350. DOI: https://doi.org/10.1016/j.gsf.2014.01.002

[45] Pollock, J. C., Hibbard, J. P., van Staal, C. R., 2009. Early Ordovician rifting of Avalonia and birth of the Rheic Ocean: U–Pb detrital zircon constraints from Newfoundland. Tectonophysics, 479(1-2), 231-248. DOI: https://doi.org/10.1016/j.tecto.2009.08.002